

Estimating the degree of non-Markovianity using machine learning

Felipe F. Fanchini,^{1,*} Göktuğ Karpat,² Daniel Z. Rossatto,³ Ariel Norambuena,⁴ and Raúl Coto⁴

¹*Faculdade de Ciências, UNESP - Universidade Estadual Paulista, Bauru, SP, 17033-360, Brazil*

²*Faculty of Arts and Sciences, Department of Physics, İzmir University of Economics, İzmir, 35330, Turkey*

³*Universidade Estadual Paulista (Unesp), Campus Experimental de Itapeva, 18409-010 Itapeva, São Paulo, Brazil*

⁴*Centro de Investigación DAiTA Lab, Facultad de Estudios Interdisciplinarios, Universidad Mayor, Chile*

(Dated: April 10, 2022)

In the last years, application of machine learning methods have become increasingly relevant in different fields of physics. One of the most significant subjects in the theory of open quantum systems is the study of the characterization of non-Markovian memory effects that emerge dynamically throughout the time evolution of open systems as they interact with their surrounding environment. Here we consider two well established quantifiers of the degree of memory effects, namely, the trace distance and the entanglement based measures of non-Markovianity. We demonstrate that using machine learning techniques, in particular, support vector machine algorithms, it is possible to estimate the degree of non-Markovianity in two paradigmatic open system models with very high precision. Our approach has the potential to be experimentally feasible to estimate the degree of non-Markovianity, since it requires a single or at most two rounds of state tomography.

I. INTRODUCTION

Artificial intelligence is a wide research field which aims to simulate human intelligence using certain machines which are programmed to perform human-like skills. Presently, the study of artificial intelligence encompasses several branches, such as machine learning (ML), reinforcement learning and deep learning, the former being the most prominent one. ML has recently become a crucial tool for extracting useful information from the very rapidly increasing rate of available data, and is now widely used in numerous research areas including computer science, medicine, chemistry, biology and physics [1]. In particular, supervised ML is an approach where the machine learns from data that have been already labeled. For a given classification task, these labels belong to different classes, whereas in case of a given regression task, they denote real values, e.g., outcomes of a measurement [2]. Therefore, in this way, it becomes possible to set a labeling model which can be used to predict the corresponding label of the unknown data. Recently, ML has had a remarkable impact in physics [3–5], for instance, in the fields of condensed matter physics [6–8], quantum phase transitions [9–12], and quantum information science [13–15].

Unlike the ideal isolated quantum systems that evolve unitarily in time, realistic quantum systems are in general open to interaction with an environment which gives rise to non-unitary dynamics resulting in loss of coherence [16, 17]. Understanding the physics of open quantum systems is of both fundamental and practical interest since the development of quantum technologies relies on the presence of precious quantum resources such as coherence [18, 19]. One of the principal concepts in the study of open quantum systems is the dynamical memory effects which might arise throughout the time evolution of the open system, and define non-Markovian dynamics [16]. Thanks to these memory effects, quantum systems can recover some part of the lost coherence enhancing

various tasks in quantum information science [20]. Despite the fact that, under special circumstances, evolution of open systems can be treated under Markovian approximation ignoring the memory effects, non-Markovian behavior cannot be actually overlooked in many realistic settings. In fact, the theory of non-Markovianity in the dynamics of open quantum systems has been widely explored in the recent literature from various different perspectives [21–26], and numerous means of quantifying it have been proposed [27]. In addition, the detection of memory effects in the open system dynamics has also been experimentally achieved [28–31]. More recently, ML methods have been started to be employed to study non-Markovian quantum processes [32–35].

In this work, we present a computational approach based on ML techniques to determine the degree of non-Markovianity in the dynamics of open systems. The proposed approach requires prior knowledge only about the type of the dominant decoherence process that our system of interest undergoes. In other words, we will assume that we know the underlying dynamical process, but we have no information about the characteristic model parameters defining the Markovian or non-Markovian nature of this process. Here, we consider two distinct well established quantifiers of memory effects for our analysis, namely, the trace distance [36] and the entanglement based measures [37]. Although capturing the signatures of non-Markovian behavior has been possible in some experiment in the recent literature [31], accurate determination of the degree of non-Markovianity remains challenging for a wide variety of experimental setups, since in general it would require a large number of rounds of quantum state tomography to be successfully performed on the open system. Moreover, depending on the considered measure in an experiment, one would need to deal with the time evolution of a pair of different initial states or even introduce an ancillary system that needs to be protected from the destructive environmental effects. Consequently, the main motivation of our study is to simplify the experimental determination of the non-Markovianity quantifiers with the help of a ML algorithm. In particular, we show that a support vector machines (SVM) based model, precisely assesses the degree

* fanchini@fc.unesp.br

of non-Markovianity of two paradigmatic quantum processes, i.e., phase damping (PD) and amplitude damping (AD), with only a single or at most two rounds of quantum state tomography. At the same time, our results provide a proof of principle that the non-Markovianity quantifiers can be precisely estimated with the assistance of ML techniques.

This manuscript is organized as follows. In Sec. II, we introduce the quantifiers of non-Markovianity considered in our work. Sec. III includes the open system models we take into account in our analysis. In Sec. IV, we briefly review the ML model we use in our analysis. We present our main results in Sec. V and we conclude in Sec. VI.

II. QUANTIFYING NON-MARKOVIANITY

In this section, we intend to briefly discuss how the non-Markovian memory effects in the dynamics of open quantum systems can be quantified. In our investigation, we consider two well-known measures of non-Markovianity [36, 37] that can be related to information dynamics between the open system and its environment from different perspectives [29].

Let us first introduce the trace distance measure which is constructed upon the distinguishability of an arbitrary pair of quantum states represented by the density operators ρ_1 and ρ_2 . The trace distance between these two states can be written as $D(\rho_1, \rho_2) = \frac{1}{2} \text{Tr}|\rho_1 - \rho_2|$, with $|A| = \sqrt{A^\dagger A}$. Since a temporary increase of distinguishability, measured with the trace distance, throughout the open system dynamics can be interpreted as a backflow of information from the environment to the open system, signatures of memory effects are signalled when $dD/dt > 0$. On the other hand, if the trace distance monotonically decreases or remains constant during the dynamics, that is $dD/dt \leq 0$, then it means that the dynamics has no memory and thus it is Markovian. Therefore, the degree of non-Markovianity is measured by [36]

$$\mathcal{N}_D = \max_{\rho_1(0), \rho_2(0)} \int_{(dD(t)/dt) > 0} \frac{dD(t)}{dt} dt \quad (1)$$

where the optimization is performed over all possible pairs of initial states $\rho_1(0)$ and $\rho_2(0)$. As it has been suggested in the recent literature [38], in our calculations we assume that the optimal initial states are orthogonal [39] and given by the eigenstates of the Pauli operator along x direction.

The second measure that we use in our study is based on the entanglement dynamics of a bipartite quantum state, given by our system of interest and an ancilla that is isolated from the effects of the environment. Aside from the interpretation of the information flow using distinguishability, this approach is linked to the information dynamics between the open quantum system and its environment through entropic quantities [29, 37]. Specifically, let us introduce an ancilla system A , which has the same dimension as the principal open system B . Considering that the subsystem B undergoes decoherence and the ancilla A evolves trivially, a monotonic decrease in entanglement of the bipartite system AB implies that the dynamics is Markovian. However, any temporary increase in entanglement throughout the time evolution can be used

to capture the memory effects in the open system dynamics. Thus, non-Markovianity can be quantified with

$$\mathcal{N}_E = \max_{\rho_{AB}(0)} \int_{(dE(t)/dt) > 0} \frac{dE(t)}{dt} dt \quad (2)$$

where the optimization is carried out over all initial states $\rho_{AB}(0)$. Since it has been demonstrated for one qubit that the optimal value of the measure is attained for Bell states [40], we calculate it considering that the initial bipartite system AB is in one of the Bell states. We also note that any entanglement measure can be used to evaluate this measure but we choose to focus on the concurrence [41].

III. OPEN QUANTUM SYSTEM MODELS

We now introduce the paradigmatic open quantum system models that we consider to study how well one can determine the degree of non-Markovianity using ML techniques.

A. Phase Damping

Let us first consider a two-level quantum system (qubit) undergoing decoherence induced by colored dephasing noise as introduced in Ref. [42]. Suppose that the time-evolution of the qubit is described by a master equation of the form

$$\dot{\rho} = K\mathcal{L}\rho, \quad (3)$$

where \mathcal{L} is a Lindblad superoperator and ρ denotes the density operator of our system of interest. Here, the time-dependent integral operator K acts on the open system as $K\phi = \int_0^t k(t-t')\phi(t')dt'$ with $k(t-t')$ being a kernel function governing the type of memory in the environment. A master equation of the form given in Eq. (3) can arise, for instance, when one considers a time-dependent Hamiltonian

$$H(t) = \hbar \sum_{k=1}^3 \Gamma_k(t) \sigma_k, \quad (4)$$

where $\Gamma_k(t)$ are independent random variables possessing the statistics of a random telegraph signal, and σ_k are the Pauli matrices in x, y and z directions. The random variables can be expressed as $\Gamma_k(t) = \alpha_k (-1)^{n_k(t)}$, where each $n_k(t)$ has a Poisson distribution with a mean equal to $t/2\tau_k$ and α_k is a coin-flip random variable with the possible values $\pm\alpha_k$.

To obtain a solution for the density operator ρ of the open system qubit, one can directly use the von Neumann equation given by $\dot{\rho} = -(i/\hbar)[H, \rho]$, then it reads

$$\rho(t) = \rho(0) - i \int_0^t \sum_k \Gamma_k(s) [\sigma_k, \rho(s)] ds. \quad (5)$$

Substituting Eq. (5) back into the von Neumann equation and evaluating the stochastic average, one gets

$$\dot{\rho}(t) = - \int_0^t \sum_k e^{-(t-t')/\tau_k} \alpha_k^2 [\sigma_k, [\sigma_k, \rho(t')]] dt', \quad (6)$$

using the correlation functions of the random telegraph signals $\langle \Gamma_j(t)\Gamma_k(t') \rangle = \alpha_k^2 \exp(-|t-t'|/\tau_k)\delta_{jk}$, which define the memory kernel. In Ref. [42], it has also been shown that under the condition that the noise acts only in a single direction, i.e., when two of the α_k vanish, dynamics generated by Eq. (6) is completely positive. In fact, if $\alpha_3 = 1$ and $\alpha_1 = \alpha_2 = 0$, then the open system undergoes decoherence induced by a colored dephasing noise. In this case, the Kraus operators describing the dynamics of the open system are given by

$$M_1(\nu) = \sqrt{[1 + \Lambda(\nu)]/2}\mathbb{I}, \quad (7)$$

$$M_2(\nu) = \sqrt{[1 - \Lambda(\nu)]/2}\sigma_3, \quad (8)$$

where $\Lambda(\nu) = e^{-\nu}[\cos(\mu\nu) + \sin(\mu\nu)/\mu]$, $\mu = \sqrt{(4\tau)^2 - 1}$, $\nu = t/2\tau$ is the dimensionless time and \mathbb{I} denotes the identity operator. Particularly, the dynamics of the open system can be expressed using the operator-sum representation as

$$\rho(\nu) = \sum_{i=1}^2 M_i(\nu)\rho(0)M_i^\dagger(\nu). \quad (9)$$

We note that the parameter τ controls the degree of memory effects responsible for the emergence of non-Markovianity, that is, as $\tau < 1/4$ gives a Markovian time evolution, $\tau > 1/4$ implies a non-Markovian dynamics for the open system. For further details about the physical relevance of the considered model in this part, interested readers might refer to Ref. [42].

B. Amplitude Damping

We will now consider a resonantly driven qubit under the influence of an AD channel, which is modelled as a bosonic reservoir at zero temperature [43–47]. The dynamics for this configuration is described by the Hamiltonian ($\hbar = 1$)

$$H = \omega_0\sigma_+\sigma_- + \Omega(\sigma_+e^{-i\omega_L t} + \sigma_-e^{i\omega_L t}) + \sum_k \omega_k a_k^\dagger a_k + \sum_k (g_k^* \sigma_+ a_k + g_k \sigma_- a_k^\dagger), \quad (10)$$

where $\sigma_+ = \sigma_-^\dagger = |e\rangle\langle g|$, and $|e\rangle$ ($|g\rangle$) corresponds to the excited (ground) state of the qubit with transition frequency ω_0 . The external driving field strength and its frequency are denoted by Ω and $\omega_L = \omega_0$, respectively, while a_k^\dagger (a_k) is the creation (annihilation) operator of the k -th reservoir mode with frequency ω_k . Finally g_k is the coupling strength between the qubit and the k -th mode. The dissipation kernel is given by

$$f(t) = \sum_k |g_k|^2 e^{-i(\omega_k - \omega_0)t} = \int_0^\infty d\omega J(\omega) e^{-i(\omega - \omega_0)t}, \quad (11)$$

with $J(\omega)$ being the spectral density of the reservoir. Without loss of generality, we assume the qubit resonantly couples to a reservoir with a Lorentzian spectral density [16, 43–48]

$$J(\omega) = \left(\frac{\gamma_0}{2\pi}\right) \frac{\lambda^2}{(\omega - \omega_0)^2 + \lambda^2}, \quad (12)$$

in which the spectral width (twice the coupling λ) is related to the correlation time of the reservoir $\tau_B \approx 1/\lambda$, whereas γ_0 is connected to the time scale in which the state of the system changes $\tau_R \approx 1/\gamma_0$ [16]. For this spectral density and considering no external driving field, the open system dynamics is essentially Markovian within the weak coupling regime, which corresponds to $\tau_R > 2\tau_B$ ($\lambda > 2\gamma_0$). By contrast, the dynamics exhibits non-Markovian features within the strong coupling regime where $\lambda < 2\gamma_0$.

When the spectral density is Lorentzian, the interaction of the qubit with its genuine environment can be exactly modeled by an equivalent ‘Markovian’ description, in which the qubit itself is coupled to a damped harmonic oscillator (auxiliary pseudomode described by the bosonic operators b and b^\dagger), which is initially in the vacuum state. Relationship between the original environment variables and the pseudomode ones is well established and the details can be found in Ref. [49]; besides it is worth emphasizing the pseudomode is a mathematical construction and, strictly, does not exist physically. Here, the system-pseudomode dynamics, described by the density operator ϱ_t , is given by the following master equation in a frame rotating with the driving field frequency [43]

$$\dot{\varrho}_t = -i[\mathcal{H}, \varrho_t] + \mathcal{L}_b \varrho_t, \quad (13)$$

with

$$\mathcal{H} = \Omega(\sigma_+ + \sigma_-) + \sqrt{\lambda\gamma_0/2}(\sigma_+ b + b^\dagger \sigma_-), \quad (14)$$

$$\mathcal{L}_b \varrho_t = \lambda(2b\varrho_t b^\dagger - b^\dagger b\varrho_t - \varrho_t b^\dagger b). \quad (15)$$

The qubit dynamics is obtained by taking the partial trace over the harmonic oscillator degrees of freedom, i.e., $\rho_t = \text{Tr}_b[\varrho_t]$. We remark that, up to our best knowledge, Eq. (13) does not have a closed-form solution for ρ_t in the general case. However, when there is no external driving field, $\Omega = 0$, open system dynamics of the qubit is then given by [16, 48]

$$\rho_t = \begin{pmatrix} \rho_{ee}^0 P_t & \rho_{eg}^0 \sqrt{P_t} \\ \rho_{ge}^0 \sqrt{P_t} & \rho_{gg}^0 + \rho_{ee}^0 (1 - P_t) \end{pmatrix}, \quad (16)$$

where $P_t = e^{-\lambda t}[\cos(dt/2) + (\lambda/d)\sin(dt/2)]^2$ with $d = \sqrt{2\gamma_0\lambda - \lambda^2}$, and ρ_{ij}^0 denotes the initial state elements.

IV. MACHINE LEARNING

There are now myriads of learning models available in the literature [2], each of which are suitable for a particular problem. Since we will perform our calculations using SVM throughout this study, it is instructive to introduce the main aspects of this computational approach.

A. Support Vector Machines

One of the most well understood ML models is SVM [50]. This model can be used for classification (SVC) [51–54] and regression (SVR) [55–57]. Moreover, it has been recently extended to the quantum regime [58–61]. In general lines, SVC

is a class of algorithms aiming to find a hyperplane that splits the dataset based on the different classes. Therefore, predicting the label of unknown data is relatively easy, since it only depends on where the data samples fall with respect to the hyperplane. The way a hyperplane can be defined is not unique, and thus, SVC sets the maximum-margin, i.e. maximizing the distance between the hyperplane and some of the boundary training data, which are the data samples that are close to the edge of the class. These particular samples are known as support vectors (SVs). Since SVs are a subset of the training dataset, this model is suitable for situations where the number of training data samples is small as compared to the dimension of the features vector. Moreover, once the model has fitted the training dataset, it can be used as a decision function that predicts new samples, without holding in memory the training dataset. For a non-linearly-separated dataset, it is possible to define a clever kernel function that takes the samples to a higher dimensional space, where they are linearly separated. Although we have only provided an intuitive representation for SVC, here we give a brief mathematical description for SVR which will be our main tool in the rest of this manuscript.

SVR delivers the tools for finding a function $f(\mathbf{x})$ that fits the training dataset $\{\mathbf{x}_i, y_i\}$, where $\mathbf{x}_i \in \mathbb{R}^d$, and $y_i \in \mathbb{R}$ labels each sample. Note that d stands for the dimension of the features vector. For illustration, we focus on a linear function $f(\mathbf{x}) = \mathbf{w} \cdot \mathbf{x} + b$, with $\mathbf{w} \in \mathbb{R}^d$ and $b \in \mathbb{R}$ being fitting parameters. For ϵ -SVR [50], deviations of $f(\mathbf{x}_i)$ from the labeled data (y_i) must be smaller than ϵ , i.e. $|f(\mathbf{x}_i) - y_i| \leq \epsilon$. Moreover, the desired function must be as flat as possible but can also include some errors. Therefore, the optimization problem can actually be stated as [2, 50, 57]

$$\begin{aligned} & \text{minimize} && \frac{1}{2} \|\mathbf{w}\|^2 + C \sum_i (\xi_i + \xi_i^*) & (17) \\ & \text{subjected to} && \begin{cases} y_i - \mathbf{w} \cdot \mathbf{x}_i - b \leq \epsilon + \xi_i \\ \mathbf{w} \cdot \mathbf{x}_i + b - y_i \leq \epsilon + \xi_i^* \\ \xi_i, \xi_i^* \geq 0 \end{cases} & (18) \end{aligned}$$

where ξ_i, ξ_i^* are slack variables and the condition $C > 0$ sets the tolerance for deviations larger than ϵ .

V. MAIN RESULTS

We commence our analysis considering what we refer to as pure PD and AD channels, where a pure channel means that no external driving field is present. For each one of these models, in order to generate a database for the training process, we calculate the time evolution of the open system and use the aforementioned measures to quantify the degree of non-Markovianity for model parameters, i.e., λ and τ . We consider a wide range of parameter values that define the two processes. In particular, in case of the AD channel, we train our algorithm taking the coupling parameter λ in the range $[0.1, 3.0]$ with a step size equal to 10^{-3} , which generates a uniformly distributed training data with 2900 samples. On the other hand, for the PD channel, the parameter τ is varied in the range $[0.1, 0.5]$ with a step size equal to 10^{-4} , which results in a uniformly distributed training data with 4000 samples.

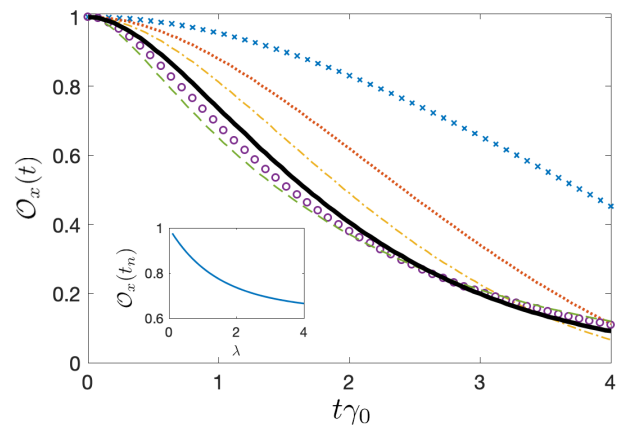


FIG. 1. Dynamics of the observable $O_x(t)$ for different coupling strengths $\lambda = 0.1, 0.5, 1.0, 3.0, 5.0$. The thick solid line is the separation curve between Markovian and non-Markovian dynamics, i.e., $\lambda = 2.0$. In the inset, we show how $O_x(1/\gamma_0)$ changes with λ .

Hereafter, we name each sample of these databases as λ_n and τ_n . It is worth to note that we actually train two independent regressors, one for each channel, but we will discuss both of them in parallel because of the identical procedure.

Next, we calculate the observables O_x , O_y , and O_z at a fixed time t^* in the dynamics where

$$\mathcal{O}_k = \text{Tr}[\sigma_k \rho(t^*)], \quad (19)$$

with σ_k being the three Pauli spin operators in the x , y and z directions. We should emphasize that the expectation values for \mathcal{O}_k are calculated for all λ_n and τ_n individually at each fixed time point t^* . Therefore, our database now contains, for each model parameter, the expectations values $O_x(t^*)$, $O_y(t^*)$, and $O_z(t^*)$ as the *features* and the degree of non-Markovianity is our *target* value. We note that the experimental determination of these expectation values can be realized with a single quantum state tomography performed at each time t^* . To summarize, we introduce to our learner a set of examples with features and their known respective targets, and our main objective is to train a regressor that will be able to determine the degree of non-Markovianity, given a pure decoherence process (without external fields), using the information contained in the expectation values.

We would like to first point out that, in case of the pure channels, depending on the time t^* , each expectation value $\mathcal{O}_k(t)$, can have a unique correspondence with each λ_n and τ_n for AD and PD, respectively. For illustrative purpose, we show in Fig. 1 the time evolution of $O_x(t)$ for different values of λ for pure AD channel. It is straightforward to note that one can find an optimal time t_c , (for example, in this case, around $1/\gamma_0$), at which the curves corresponding the Markovian and non-Markovian dynamics are well separated, depending on whether they are above or below the thick solid line ($\lambda = 2.0$). This suggests that a single state tomography, in a well determined time t_c , is sufficient to estimate the degree of non-Markovianity. For example, if $t\gamma_0 = 1$, for each value of λ , we have a precise and distinct value of $O_x(t)$. In

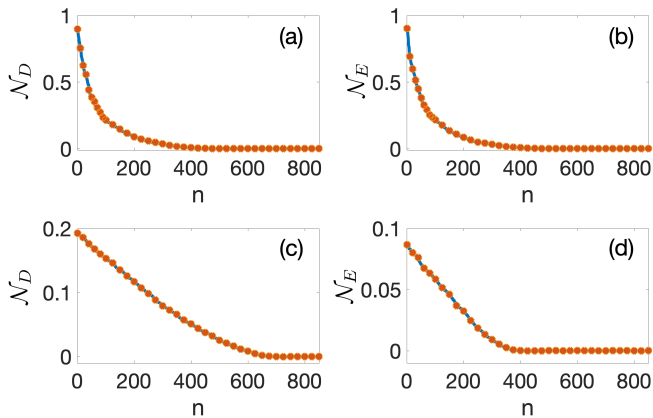


FIG. 2. Comparison of the estimated (circles) and theoretical values of the degree of non-Markovianity for pure decoherence channels. The plots (a) and (b) display the results for the trace distance \mathcal{N}_D and the entanglement based \mathcal{N}_E measures in case of pure AD channel, respectively. On the other hand, the plots (c) and (d) show the outcomes of the same investigation in case of pure PD channel.

the inset of Fig. 1 (assuming $t\gamma_0 = 1$) we show that there is an optimal region where, even for small variations in λ , the change in $\mathcal{O}_x(t_c)$ is significant. This is crucial to determine the best t_c to be used in an experiment. Indeed, we need to choose a time t_c that increases the accuracy of the ML algorithm but, at the same time, keep sparse the expectation values as a function of λ . For example, examining Fig. 1, we see that one could choose $t\gamma_0 = 0.5$ but, in this case, a high precision measurement is necessary since $\mathcal{O}_x(t)$ varies not much, i.e., from approximately 0.8 to 1.0 as λ ranges from 0.1 to 3.0. This imposes a balance between the experimental precision of the measurements and the accuracy of the ML algorithm.

An important aspect of the application of ML algorithms is the concept of data normalization. Here, we also employ the procedure of feature standardization which makes the values of each feature in the dataset to have zero mean and unit variance. Such a treatment can in general speed up the algorithm convergence [62] while increasing the accuracy of method. Thus, for each set of observables, we calculate their mean value and variance, and transform the data as

$$\tilde{\mathcal{O}}_k^n = (\mathcal{O}_k^n - u_k)/s_k, \quad (20)$$

where \mathcal{O}_k^n is a specific data of \mathcal{O}_k (that is, for a particular λ_n or τ_n), u_k is the mean value of \mathcal{O}_k observable, and s_k is the standard deviation of \mathcal{O}_k . We remark that this simple procedure can actually enhance the accuracy of the estimation up to one order of magnitude.

We now turn our attention to the results on the estimation of the degree of non-Markovianity in pure AD and PD channels, which are generated by the regressor we trained. From this point on, out of the whole database we have produced, we will keep always 70% of the data (which are randomly chosen) to train the SVR, and we will reserve the remaining 30% of the data to test the performance of the regressor. Note that this is a standard procedure when working with SVR, but we should also remark that the choice of these percentages can be

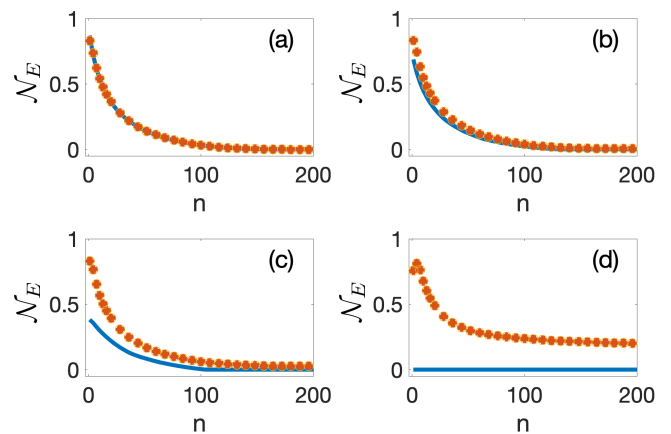


FIG. 3. Comparison between the predicted (circles) and theoretical values of the degree of non-Markovianity of the AD channel, as measured by the entanglement based measure \mathcal{N}_E , for increasing values of the field strength Ω from plot (a) to plot (f). Here, the regressor is trained with the data generated for the pure AD channel.

adjusted depending on the problem to improve the prediction accuracy. In Fig. 2, we show the degree of non-Markovianity predicted with our SVR model (orange circles) and the theoretical ones (blue solid line) in case of pure decoherence channels, considering both the trace distance \mathcal{N}_D and entanglement based \mathcal{N}_E measures of non-Markovianity. Here, in the generation of the dataset, the expectation values $\mathcal{O}_k(t)$ are calculated at the fixed time $t_c = 3/\gamma_0$ ($t_c = 3$) for AD (PD), which optimize the separation among the values of the three observables. We also note that the theoretical data is arranged in decreasing order and we limit the number of the estimated non-Markovianity values in the figure merely for illustrative purposes. Specifically, whereas Fig. 2a and Fig. 2b respectively show our findings for \mathcal{N}_D and \mathcal{N}_E for the AD channel, Fig. 2c and Fig. 2d display the results of the same analysis for the PD channel. It then becomes clear that our ML algorithm can estimate the degree of non-Markovianity with a very high precision. Indeed, the mean errors for AD and the PD channels are given by 7×10^{-4} and 2×10^{-4} for the trace distance measure, and 9×10^{-4} and 9×10^{-5} for the entanglement based measure, respectively. Therefore, for pure decoherence channels, a single tomography should be sufficient to accurately estimate the degree of memory effects.

At this point, it is important to mention that the above results on the AD channel clearly depend on the knowledge of the parameter γ_0 so that the timescale of t_c can be reliably determined and our approach can be used in an experiment. If the parameter γ_0 is unknown in the considered setting, it has been recently addressed in Ref. [63] that the noise spectrum of any environment surrounding a qubit can be accurately extracted by training a deep neural network (long short-term memory network) with usual time-dynamics measurements on qubits, e.g., the two-pulse ‘Hahn’ echo curves.

Motivated by the results we have obtained for pure decoherence channels, we would like to apply our computational approach to a natural extension of the studied problem, that is,

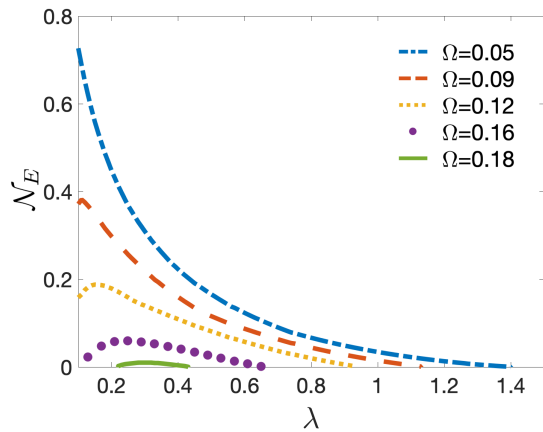


FIG. 4. The degree of non-Markovianity as quantified with the entanglement based measure \mathcal{N}_E as a function of the coupling strength λ for different values of external driving field strength Ω .

we ask the question of what would be the consequences of an external driving field affecting the open system? This problem is certainly more involved as compared to pure decoherence since the external field induces extra oscillations in the evolution of the expectation values \mathcal{O} , which could be mistaken as a signature of non-Markovianity by the regressor. In this part, we choose to limit our analysis to the non-Markovianity of the AD channel quantified through the entanglement based measure \mathcal{N}_E . We will now assume an external driving $\Omega \neq 0$ in Eq. (10) and we follow the procedure that we have used to obtain the results presented in Fig. 2. In fact, our first question here is: given a regressor that is trained to work with pure AD channel, how precisely is it able to estimate the degree of non-Markovianity in the presence of an external field? To answer this question we show in Fig. 3 the comparison between the estimated (by a regressor trained for pure AD channel) and the theoretical non-Markovianity results when the external field is non-zero for the AD channel. In the plots displayed from Fig. 3a to Fig. 3d, we consider the external field strength Ω values to be 0.01, 0.05, 0.09, and 0.20 in respective increasing order, which in turn result in mean errors given by 1.7×10^{-3} , 1.9×10^{-2} , 5.5×10^{-2} , and 0.21. As can be seen comparing the predicted and theoretical non-Markovianity values, the results are satisfactory only for small perturbations, and as the driving strength increases, the regressor no longer works.

Our findings in Fig. 3 agree with what we expected since the effects induced by the external driving can significantly alter the time evolution of the expectation values $\mathcal{O}_x(t)$, $\mathcal{O}_y(t)$, and $\mathcal{O}_z(t)$. It is also important to emphasize that revivals in the dynamics of the expectations values do not necessarily imply that the time evolution is non-Markovian. Actually, the external field Ω suppresses the memory effects in the open system dynamics despite the fact that it causes oscillations in the dynamics of the expectation values. Fig. 4 demonstrates this situation, i.e., while the field strength Ω increases, non-Markovianity \mathcal{N}_E decreases, tending to zero even for small values of Ω . This behavior is the cause of the inaccuracy of the non-Markovianity estimated by the SVR algorithm in Fig. 3.

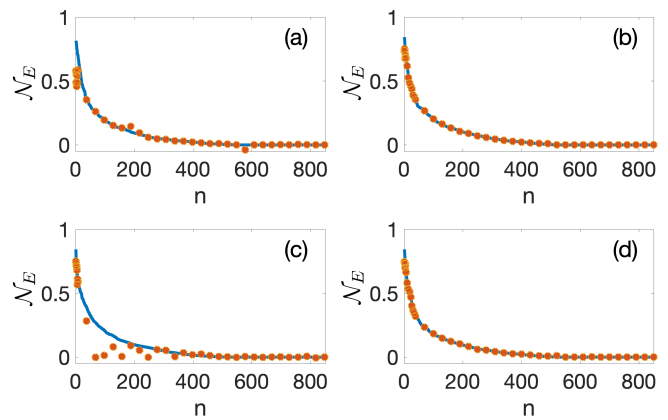


FIG. 5. Comparison between the estimated (circles) and theoretical values of the degree of non-Markovianity for the AD channel with external field, as measured by the entanglement based measure \mathcal{N}_E , where the regressor is trained taking into account the external field. While the plots in (a) and (c) are generated considering a single state tomography at a fixed time during the dynamics, the results in the plots (b) and (d) are obtained taking into account two tomographies.

In order to enhance the predictive power of our SVR based ML algorithm, the natural solution is to train the regressor taking into account the existence of the external field Ω . Thus, we now train our algorithm assuming that the coupling strength λ takes values in the range $[0.1, 3.0]$, with a step size equal to 10^{-2} , and additionally, we consider a set of values for the drive parameter Ω (ranging from 0.01 to 0.5), which generates an uniformly distributed training data with 290 samples for each Ω . In Fig. 5, we present the predictions of our regressor now trained in the presence of the external field. In particular, Fig. 5a and Fig. 5c present a comparison of the theoretical and the estimated results of the non-Markovianity measure \mathcal{N}_E using the values of the expectation values $\mathcal{O}_x(t_c)$, $\mathcal{O}_y(t_c)$, and $\mathcal{O}_z(t_c)$ at fixed times $t_c = 3/\gamma_0$ and $t_c = 5/\gamma_0$, respectively. Note that for each case, the experimental implementation requires a single state tomography performed at time t_c . As can be seen from these plots, we obtain a better result for $t_c = 3/\gamma_0$ as compared to $t_c = 5/\gamma_0$ (mean error for these two cases are 2.6×10^{-3} and 1.3×10^{-2} , respectively). Next, in order to further improve the estimation efficiency of our SVR algorithm, we let our regressor to have access to more information, which means that we train it using the values of $\mathcal{O}_x(t_c)$, $\mathcal{O}_y(t_c)$, and $\mathcal{O}_z(t_c)$ at two fixed times t_{c_1} and t_{c_2} . The outcomes of our analysis in this case are shown in Fig. 5b and Fig. 5d. Particularly, Fig. 5b includes the results of the comparison between the estimated and the theoretical values of the non-Markovianity for the AD channel with external drive when two state tomographies are performed at times $t_{c_1} = 3/\gamma_0$ and $t_{c_2} = 6/\gamma_0$. On the other hand, in Fig. 5d, the outcomes of the same analysis are given when the measurement times are $t_{c_1} = 5/\gamma_0$ and $t_{c_2} = 10/\gamma_0$. Consequently, we see that two quantum state tomographies at fixed times spaced by the intervals either $3/\gamma_0$ or $5/\gamma_0$ should be sufficient to precisely estimate the degree of non-Markovianity with mean errors 1.2×10^{-3} and 1.3×10^{-3} , respectively.

VI. CONCLUSION

In summary, we have introduced an experimentally friendly approach, which utilizes ML techniques based on SVR, to estimate the degree of memory effects in the dynamics of open quantum systems. In particular, we have first considered the trace distance and entanglement based measures of non-Markovianity and demonstrated that, in case of pure AD and PD channels, a single quantum state tomography should be sufficient to estimate the value of non-Markovianity measures very precisely. Next, we have focused on AD channel also taking into account an external drive on the open system. We have demonstrated that even though the regressor trained with the pure AD data can estimate the degree of non-Markovianity relatively well for small values of the external drive strength, as the drive parameter increases, our method no longer works due to the extra oscillations induced on the expectation values

\mathcal{O} by the external drive. We have then shown that once our regressor is trained with the data provided by the AD channel dynamics, including the external drive, it becomes possible to precisely estimate the degree of non-Markovianity with at most two rounds of state tomography.

VII. ACKNOWLEDGEMENTS

F. F. F. acknowledges support from Fundação de Amparo à Pesquisa do Estado de São Paulo (FAPESP), project number 2019/05445-7. G. K. is supported by the BAGEP Award of the Science Academy, the TUBA-GEBIP Award of the Turkish Academy of Sciences, and also by the Technological Research Council of Turkey (TUBITAK) under Grant No. 117F317. A.N. acknowledges support from Universidad Mayor through the Postdoctoral fellowship. R.C. acknowledges support from Fondecyt Iniciación No. 11180143.

-
- [1] M. I. Jordan and T. M. Mitchell, “Machine learning: Trends, perspectives, and prospects,” *Science* **349**, 255–260 (2015).
 - [2] Fabian Pedregosa, Gaël Varoquaux, Alexandre Gramfort, Vincent Michel, Bertrand Thirion, Olivier Grisel, Mathieu Blondel, Peter Prettenhofer, Ron Weiss, Vincent Dubourg, Jake Vanderplas, Alexandre Passos, David Cournapeau, Matthieu Brucher, Matthieu Perrot, and Édouard Duchesnay, “Scikit-learn: Machine learning in python,” *Journal of Machine Learning Research* **12**, 2825–2830 (2011).
 - [3] Vedran Dunjko and Hans J Briegel, “Machine learning & artificial intelligence in the quantum domain: a review of recent progress,” *Reports on Progress in Physics* **81**, 074001 (2018).
 - [4] Pankaj Mehta, Marin Bukov, Ching-Hao Wang, Alexandre G.R. Day, Clint Richardson, Charles K. Fisher, and David J. Schwab, “A high-bias, low-variance introduction to machine learning for physicists,” *Physics Reports* **810**, 1 – 124 (2019), a high-bias, low-variance introduction to Machine Learning for physicists.
 - [5] Giuseppe Carleo, Ignacio Cirac, Kyle Cranmer, Laurent Daudet, Maria Schuld, Naftali Tishby, Leslie Vogt-Maranto, and Lenka Zdeborová, “Machine learning and the physical sciences,” *Rev. Mod. Phys.* **91**, 045002 (2019).
 - [6] Luca M. Ghiringhelli, Jan Vybiral, Sergey V. Levchenko, Claudia Draxl, and Matthias Scheffler, “Big data of materials science: Critical role of the descriptor,” *Phys. Rev. Lett.* **114**, 105503 (2015).
 - [7] Giacomo Torlai and Roger G. Melko, “Learning thermodynamics with boltzmann machines,” *Phys. Rev. B* **94**, 165134 (2016).
 - [8] Giuseppe Carleo and Matthias Troyer, “Solving the quantum many-body problem with artificial neural networks,” *Science* **355**, 602–606 (2017).
 - [9] Juan Carrasquilla and Roger G. Melko, “Machine learning phases of matter,” *Nature Physics* **13**, 431–434 (2017).
 - [10] Pedro Ponte and Roger G. Melko, “Kernel methods for interpretable machine learning of order parameters,” *Phys. Rev. B* **96**, 205146 (2017).
 - [11] Ke Liu, Jonas Greitemann, and Lode Pollet, “Learning multiple order parameters with interpretable machines,” *Phys. Rev. B* **99**, 104410 (2019).
 - [12] Askery Canabarro, Felipe Fernandes Fanchini, André Luiz Malvezzi, Rodrigo Pereira, and Rafael Chaves, “Unveiling phase transitions with machine learning,” *Phys. Rev. B* **100**, 045129 (2019).
 - [13] Giacomo Torlai, Guglielmo Mazzola, Juan Carrasquilla, Matthias Troyer, Roger Melko, and Giuseppe Carleo, “Neural-network quantum state tomography,” *Nature Physics* **14**, 447–450 (2018).
 - [14] Askery Canabarro, Samurá Brito, and Rafael Chaves, “Machine learning nonlocal correlations,” *Phys. Rev. Lett.* **122**, 200401 (2019).
 - [15] Raban Iten, Tony Metger, Henrik Wilming, Lídia del Rio, and Renato Renner, “Discovering physical concepts with neural networks,” *Phys. Rev. Lett.* **124**, 010508 (2020).
 - [16] H.-P. Breuer and F. Petruccione, *The Theory of Open Quantum Systems* (Oxford University Press, Oxford, 2007).
 - [17] Angel Rivas and Susana F Huelga, *Open quantum systems* (Springer, 2012).
 - [18] T. Baumgratz, M. Cramer, and M. B. Plenio, “Quantifying coherence,” *Phys. Rev. Lett.* **113**, 140401 (2014).
 - [19] Alexander Streltsov, Gerardo Adesso, and Martin B. Plenio, “Colloquium: Quantum coherence as a resource,” *Rev. Mod. Phys.* **89**, 041003 (2017).
 - [20] B. Bylicka, D. Chruściński, and S. Maniscalco, “Non-markovianity and reservoir memory of quantum channels: a quantum information theory perspective,” *Scientific Reports* **4**, 5720 (2014).
 - [21] Heinz-Peter Breuer, Elsi-Mari Laine, Jyrki Piilo, and Bassano Vacchini, “Colloquium: Non-markovian dynamics in open quantum systems,” *Rev. Mod. Phys.* **88**, 021002 (2016).
 - [22] Li Li, Michael J.W. Hall, and Howard M. Wiseman, “Concepts of quantum non-markovianity: A hierarchy,” *Physics Reports* **759**, 1 – 51 (2018).
 - [23] C.-F. Li, G.-C. Guo, and J. Piilo, “Non-markovian quantum dynamics: What is it good for?” *Europhys. Lett.* **128**, 30001 (2020).
 - [24] Felipe F. Fanchini, Göktuğ Karpat, Leonardo K. Castelano, and Daniel Z. Rossatto, “Probing the degree of non-markovianity for independent and common environments,” *Phys. Rev. A* **88**, 012105 (2013).

- [25] G. Karpat, Jyrki Piilo, and Sabrina Maniscalco, “Controlling entropic uncertainty bound through memory effects,” *EPL (Europhysics Letters)* **111**, 50006 (2015).
- [26] Carole Addis, Göktuğ Karpat, Chiara Macchiavello, and Sabrina Maniscalco, “Dynamical memory effects in correlated quantum channels,” *Phys. Rev. A* **94**, 032121 (2016).
- [27] Ángel Rivas, Susana F Huelga, and Martin B Plenio, “Quantum non-markovianity: characterization, quantification and detection,” *Rep. Prog. Phys.* **77**, 094001 (2014).
- [28] Bi-Heng Liu, Li Li, Yun-Feng Huang, Chuan-Feng Li, Guang-Can Guo, Elsi-Mari Laine, Heinz-Peter Breuer, and Jyrki Piilo, “Experimental control of the transition from markovian to non-markovian dynamics of open quantum systems,” *Nat. Phys.* **7**, 931–934 (2011).
- [29] F. F. Fanchini, G. Karpat, B. Çakmak, L. K. Castelano, G. H. Aguilar, O. Jiménez Farías, S. P. Walborn, P. H. Souto Ribeiro, and M. C. de Oliveira, “Non-markovianity through accessible information,” *Phys. Rev. Lett.* **112**, 210402 (2014).
- [30] S. Haseli, G. Karpat, S. Salimi, A. S. Khorashad, F. F. Fanchini, B. Çakmak, G. H. Aguilar, S. P. Walborn, and P. H. Souto Ribeiro, “Non-markovianity through flow of information between a system and an environment,” *Phys. Rev. A* **90**, 052118 (2014).
- [31] C.-F. Li, G.-C. Guo, and J. Piilo, “Non-markovian quantum dynamics: What is it good for?” *Europhys. Lett.* **128**, 30001 (2020).
- [32] Leonardo Bianchi, Edward Grant, Andrea Rocchetto, and Simone Severini, “Modelling non-markovian quantum processes with recurrent neural networks,” *New Journal of Physics* **20**, 123030 (2018).
- [33] Sally Shrapnel, Fabio Costa, and Gerard Milburn, “Quantum markovianity as a supervised learning task,” *International Journal of Quantum Information* **16**, 1840010 (2018).
- [34] I. A. Luchnikov, S. V. Vintskevich, D. A. Grigoriev, and S. N. Filippov, “Machine learning non-markovian quantum dynamics,” *Phys. Rev. Lett.* **124**, 140502 (2020).
- [35] Dario Poletti Chu Guo, Kavan Modi, “Tensor network based machine learning of non-markovian quantum processes,” (2020), [arXiv:2004.11038](https://arxiv.org/abs/2004.11038).
- [36] Heinz-Peter Breuer, Elsi-Mari Laine, and Jyrki Piilo, “Measure for the degree of non-markovian behavior of quantum processes in open systems,” *Phys. Rev. Lett.* **103**, 210401 (2009).
- [37] Ángel Rivas, Susana F. Huelga, and Martin B. Plenio, “Entanglement and non-markovianity of quantum evolutions,” *Phys. Rev. Lett.* **105**, 050403 (2010).
- [38] Carole Addis, Bogna Bylicka, Dariusz Chruściński, and Sabrina Maniscalco, “Comparative study of non-markovianity measures in exactly solvable one- and two-qubit models,” *Phys. Rev. A* **90**, 052103 (2014).
- [39] Steffen Wißmann, Antti Karlsson, Elsi-Mari Laine, Jyrki Piilo, and Heinz-Peter Breuer, “Optimal state pairs for non-markovian quantum dynamics,” *Phys. Rev. A* **86**, 062108 (2012).
- [40] Alaor Cervati Neto, Göktuğ Karpat, and Felipe Fernandes Fanchini, “Inequivalence of correlation-based measures of non-markovianity,” *Phys. Rev. A* **94**, 032105 (2016).
- [41] Scott Hill and William K. Wootters, “Entanglement of a pair of quantum bits,” *Phys. Rev. Lett.* **78**, 5022–5025 (1997).
- [42] Sonja Daffer, Krzysztof Wódkiewicz, James D. Cresser, and John K. McIver, “Depolarizing channel as a completely positive map with memory,” *Phys. Rev. A* **70**, 010304 (2004).
- [43] S. J. Whalen and H. J. Carmichael, “Time-local Heisenberg-Langevin equations and the driven qubit,” *Phys. Rev. A* **93**, 063820 (2016).
- [44] P. Haikka and S. Maniscalco, “Non-markovian dynamics of a damped driven two-state system,” *Phys. Rev. A* **81**, 052103 (2010).
- [45] P. Haikka, “Non-Markovian master equation for a damped driven two-state system,” *Phys. Scr.* **T140**, 014047 (2010).
- [46] H. Z. Shen, M. Qin, Xiao-Ming Xiu, and X. X. Yi, “Exact non-Markovian master equation for a driven damped two-level system,” *Phys. Rev. A* **89**, 062113 (2014).
- [47] Zhiming Huang and Haozhen Situ, “Non-markovian dynamics of quantum coherence of two-level system driven by classical field,” *Quantum Inf. Process.* **16**, 222 (2017).
- [48] B. Bellomo, R. Lo Franco, and G. Compagno, “Non-Markovian Effects on the Dynamics of Entanglement,” *Phys. Rev. Lett.* **99**, 160502 (2007).
- [49] B. M. Garraway, “Nonperturbative decay of an atomic system in a cavity,” *Phys. Rev. A* **55**, 2290–2303 (1997).
- [50] V. Vapnik, “The nature of statistical learning theory.” Springer Verlag, New York (1995).
- [51] Christopher J. C. Burges, “A tutorial on support vector machines for pattern recognition,” *Data Mining and Knowledge Discovery* **2**, 121–167 (1998).
- [52] Rainer Dietrich, Manfred Opper, and Haim Sompolinsky, “Statistical mechanics of support vector networks,” *Phys. Rev. Lett.* **82**, 2975–2978 (1999).
- [53] Sebastian Risau-Gusman and Mirta B. Gordon, “Generalization properties of finite-size polynomial support vector machines,” *Phys. Rev. E* **62**, 7092–7099 (2000).
- [54] M. Opper and R. Urbanczik, “Universal learning curves of support vector machines,” *Phys. Rev. Lett.* **86**, 4410–4413 (2001).
- [55] Schölkopf B., Bartlett P., and Williamson R. Smola A., “Support vector regression with automatic accuracy control.” In: Niklasson L., Bodén M., Ziemke T. (eds) ICANN 98. ICANN 1998. Perspectives in Neural Computing. Springer, London (1998).
- [56] Schölkopf B. and Smola A.J., *Learning with Kernels* (MIT Press., 2002).
- [57] Alex J. Smola and Bernhard Schölkopf, “A tutorial on support vector regression,” *Statistics and Computing* **14**, 199–222 (2004).
- [58] Patrick Rebstroff, Masoud Mohseni, and Seth Lloyd, “Quantum support vector machine for big data classification,” *Phys. Rev. Lett.* **113**, 130503 (2014).
- [59] Zhaokai Li, Xiaomei Liu, Nanyang Xu, and Jiangfeng Du, “Experimental realization of a quantum support vector machine,” *Phys. Rev. Lett.* **114**, 140504 (2015).
- [60] Jacob Biamonte, Peter Wittek, Nicola Pancotti, Patrick Rebentrost, Nathan Wiebe, and Seth Lloyd, “Quantum machine learning,” *Nature* **549**, 195–202 (2017).
- [61] Vojtěch Havlíček, Antonio D. Córcoles, Kristan Temme, Aram W. Harrow, Abhinav Kandala, Jerry M. Chow, and Jay M. Gambetta, “Supervised learning with quantum-enhanced feature spaces,” *Nature* **567**, 209–212 (2019).
- [62] Sergey Ioffe and Christian Szegedy, “Batch normalization: Accelerating deep network training by reducing internal covariate shift,” (2015), [arXiv:1502.03167](https://arxiv.org/abs/1502.03167).
- [63] David F. Wise, John J. L. Morton, and Siddharth Dhomkar, “Using deep learning to understand and mitigate the qubit noise environment,” (2020), [arXiv:2005.01144](https://arxiv.org/abs/2005.01144).